

Dynamic Study on Tumor Killing Activity of CD19 Chimeric Antigen Receptor-T Lymphocytes

Jiarui Guo

Kevin Poehenr, Nanjing Basis International School, Nanjing, China

Abstract. Malignant tumor is a major factor in global disease burden. In recent years, its incidence is still increasing year by year. Because of its complex etiology and the frequent recurrence and metastasis after general surgery, it brings great challenges to global public health. The emergence of new technology, that is, "Chimeric Antigen Receptor-T" immuno-therapy, has created a new era for the treatment of hematological malignant tumors, such as non-Hodgkin's lymphoma and acute B-lymphocytic leukemia. In order to evaluate the killing effect of CART tumor immuno-therapy on tumor cells more intuitively, CD19-CART cells targeting B-cell lymphoma were constructed in vitro, combined with innovative in vitro real-time cellular analysis technology. Meanwhile, it is compared with common T lymphocytes in the human body to observe their killing activity against targeted tumors. The results showed that in comparison with common T lymphocytes, CD19-CART cells constructed in this paper showed significantly enhanced killing activity for targeting tumors and a dose-dependent effect on the ratio of response to the target. Besides, CD19-CART cells constructed in this paper have a remarkable killing effect on tumor cells and adopt superior technical methods to observe the killing activity more intuitively, which provides a solid theoretical basis for the clinical application of CART cell tumor immuno-therapy technology.

Keywords: Chimeric Antigen Receptor T cell (CART), Tumor Immuno-therapy, Acute B-cell Lymphoma, Real-time Cellular Analysis (RTCA).

1. Research Background and Significance

In 2022, there will be about 4.82 million and 2.37 million new cancer cases and 3.21 million and 640,000 cancer deaths in China. The most common type of cancer is lung cancer. The incidence of other cancers including gastric cancer, liver cancer, and esophageal cancer is declining, while the incidence of colorectal cancer, prostate cancer, and breast cancer has increased.¹

For such a high incidence of cancer, its treatment has always been a difficult problem for the scientific community. However, the emergence of a new generation of tumor immuno-therapy (Chimeric Antigen Receptor-T cells, CART) has become a breakthrough therapy for different malignant tumors including lymphoma and leukemia in the 21st century.² The emergence of CART cell therapy technology has brought a new dawn to cancer patients. According to the international frontier CART research, combined with related innovative experimental techniques and detection methodologies, a chimeric antigen receptor T lymphocyte targeting CD19, a characteristic protein of B-cell lymphoma, was constructed in vitro, which kills the tumor target cells efficiently, providing a new idea for the treatment of acute B-cell malignant lymphoma in the clinic.

1.1 T Cell Activation and Tumor Immune Escape

The activation of T cells requires two signals, that is, a specific recognition signal and a co-stimulation signal. The first requires the CD3 protein complex of T cells to work together with its surface receptor TCR. TCR receptor recognizes the MHC class I molecule presenting antigen and transmits the signal from the cell surface to the cell through the ζ sub-unit of the CD3 complex, thus activating T cells.³

The co-stimulatory signals of T cells include positive co-stimulatory molecules such as CD28, CD27, ICOS, 4-1BB, OX40, and negative co-stimulatory molecules such as CTLA-4, and PD-1. CD28 and CTLA-4 co-link the ligands of CD80 and CD86, determining the activation or inhibition of T cells by their related expression levels.⁴

The activation of T cells also provides tumor cells with an opportunity for immune escape: (1) On the surface of tumor cells, PD-L1, the ligand of PD-1 molecule, is abnormally expressed, which activates PD-1 molecule on the surface of T cells, and then leads to T cell depletion, disability, and even apoptosis; (2) Tumor cells down-regulate or even completely lose MHC class I molecules on their surface, which makes it impossible for T cells to recognize them.⁵ Because CART cells specifically express antibodies and co-stimulation signals that recognize tumor surface antigens, they can effectively solve two major problems, including loss of targeting and bypassing antigen presentation. Moreover, if tumor cells down-regulate the expression of MHC class I molecules, they can be recognized and killed.

1.2 Structure of Chimeric Antigen Receptors (CAR)

The structure of CAR includes an extracellular antigen recognition domain and an intracellular signal domain. The antigen recognition domain includes the antibody domain ligand domain and TCR domain. The antigen binding domain is composed of the light chain and heavy chain of monoclonal antibodies. In addition, a flexible hinge region is connected in the middle to form a Single Chain Fragment Variable (Scfv), which is immobilized on cells to bind tumor-associated antigen,⁶ namely CD19 protein.

1.3 Development of CART Cells

The first generation CAR generally uses a CD3 ζ signal chain called "Signal 1". However, the first generation of CART cells is characterized by insufficient efficacy, which may be caused by activation-induced cell death (AICD) or lack of continuous expansion ability.⁷

The difference between the second-generation CAR and the first-generation is that an additional co-stimulation signal domain, called "Signal 2", is added to it, which optimizes the activation of T cells through the transmission of double signals. The second generation of CD19-targeting CART cells included CD3 ζ and CD28 or 4-1BB signals. Compared with the first generation of CD19-CART cells, the persistence and amplification of CART cells were enhanced in clinical trials conducted by Baylor University School of Medicine in patients with non-Hodgkin lymphoma (NHL).⁸

The signal domain of the third-generation CAR contains both the CD3 ζ domain and two co-stimulatory domains. The results of preclinical studies show that the third-generation CART cells have significantly stronger anti-tumor efficacy than the second-generation.⁹

1.4 Hematological Tumor Immuno-Therapy

In the treatment of B-cell malignant tumors, cell surface glycoprotein CD19 is the most commonly used target of B-cell tumors. Because it is not expressed in hematopoietic stem cells, its toxicity and side effects are limited to B-cell aplastic anemia, so the toxicity of this "targeted/non-tumor" is acceptable.¹⁰

At present, the clinical trial of CART targeting CD19, combining CD28 and 4-1BB co-stimulation domain is gratifying. CART19 cells can still be detected one year after adoptive transfer to patients, and the complete remission without recurrence time of two of the three patients is longer than two years.¹¹ Successive CART clinical trials targeting CD22 are also being carried out. Scientists are studying other bone marrow cell surface markers and exploring their potential as targets for T cell therapy, such as CD123, CD33, and CD44v6.¹²

It is worth mentioning that during the development of B cells, Ig κ or Ig λ light chain will be expressed, while the ratio of Ig κ^+ to Ig λ^+ in the human body ranges from 4:1 to 0.5:1. If the ratio exceeds this range, it is likely to indicate that the cell clone will become cancerous. The CART designed to target Ig light chain is different from targeting CD19, which can avoid injuring 20%-80% of B cells and plasma cells, and will not increase the risk of infection.¹³ This CART is currently undergoing clinical trials.

Generally speaking, the most potential CART cell targets for the treatment of hematological malignant tumors include CD19, CD20, CD22, and ROR1 for the treatment of B-cell malignant tumors, CD138 and BCMA (B-cell maturation antigen)¹⁴ for the treatment of plasma-cell malignant tumors, and CD123 and CD33¹⁵ for the treatment of myeloid malignant tumors. The CART cells designed in this paper selected the B cell-specific antigen CD19 with the strongest targeting, in order to achieve the best test of the killing activity of CART cells.

2. Experimental Materials and Methods

2.1 Construction of CD19 Expression Vector

2.1.1 Acquisition of CD19 Gene

Resuscitate lymphocytes, extract RNA from cells, reverse transcribed to generate cDNA template, and add corresponding primers for polymerase chain reaction (PCR) amplification. Details of the reaction procedure are shown in Table 1, and details of the linearization of the lentivirus vector are shown in Table 2.

Table 1 PCR Amplification Program

Action	Temperature	Time	
Predegeneration	95 °C	5 min	
Cyclic Degeneration	95 °C	15 s	} 34 cycles
Cyclic Annealing	56 °C	30 s	
Cyclic Extension	72 °C	35 s	
Terminal Extension	72 °C	12min	
Constant Temperature Maintenance	4 °C	30 min	

Table 2 Vector Linearized PCR Amplification Program

Action	Temperature	Time	
Predegeneration	98 °C	5 min	
Cyclic Degeneration	98 °C	15 s	} 34 cycles
Cyclic Annealing	65/75 °C	30 s	
Cyclic Extension	72 °C	90 s	
Terminal Extension	72 °C	15 min	
Constant Temperature Maintenance	4 °C	30 min	

After amplification, 1% agarose gel was prepared, the target gene was separated by nucleic acid electrophoresis, and the gel was cut and recovered. CD19 target gene product was linked with a lentivirus linearized vector by the homologous recombinant enzyme.

2.1.2 Transformation of CD19 Gene

Take a Top10 competent cell, dissolve it on ice, add CD19 recombinant plasmid, and blend lightly; After an ice bath for 30min, the cell membrane was contracted to make the recombinant plasmid adsorb on the surface of competent cells; The competent cells were incubated in 42 degrees water bath for 90 seconds to open the cell membrane channel and make the recombinant plasmid diffuse from outside to inside the membrane. Then the competent cells were quickly put back on the ice for a 3-5min ice bath.

500ul LB medium (without antibiotics) was added into the EP tube, and then the mixture was evenly stirred at 37 degrees for 220rpm/min and cultured for 45min; Competent cells were uniformly coated on ampicillin-resistant plates with sterilized coating rods, and cultured in an inverted incubator at 37 degrees for 16 hours. The next day, a single colony was picked, added to the liquid culture medium containing ampicillin resistance, and oscillated for 16 hours.

2.2 Extraction of CD19 Target Plasmid

Transfer the E. coli culture solution obtained in 2.1.2 into a 15ml centrifuge tube, 4000rpm, centrifuge for 15 minutes. Then, discard the supernatant, add 250ul solution I to the precipitate, and fully suck and mix; Solution II is added and gently upside down; Add solution III, then gently turn it up and down 6-8 times until white floccs appear, then centrifuge at 12000rpm for 10min; Supernatant was placed on the column, DNA Wash Buffer was added, centrifuged and washed repeatedly; Drop 100ul of double distilled water (preheated at 65) into the middle of the adsorption film and leave it at room temperature for 2min; 12000rpm, centrifuged for 2min, and the concentration of plasmid is finally determined with Nanodrop. The labeled plasmid was stored in a refrigerator at -20.°C

2.3 T lymphocyte Acquisition

After trimming the blood collection vessel, put it in a centrifuge, centrifuge at 3000rpm for 15 minutes, and carefully suck the upper plasma clear solution into the plasma tube after centrifugation. In addition, transfer the remaining blood cells to the 15mL centrifuge tube with a Pap straw, add 5ml DPBS to re-suspend the remaining blood cells in the blood collection vessel, and transfer them to the 15mL centrifuge tube together before using DPBS to stabilize the volume to 12mL; The mixed spinning system was beaten evenly with a pasteurized straw, then slowly spread into a 15mL centrifuge tube preloaded with 3mL Lymphoprep™ lymphocyte separation solution, and slowly placed in a table centrifuge. The speed was adjusted to 5, and the speed was adjusted to 2, with 400g centrifuging for 30 minutes. After centrifugation, the white lymphocyte layer between the lymphocyte separation liquid layer and the supernatant layer was sucked out into a new 15mL centrifuge tube by using a pasteurized straw; Add DPBS, constant volume to 15mL, upside down centrifuge tube to fully mix cells with DPBS, centrifuge 800g for 10 minutes; Discard the supernatant, add DPBS to 15mL, mix well with centrifuge tube upside down, and centrifuge 200g for 15 minutes.

2.4 Packaging of Lentivirus

293T cells were prepared in a 10cm dish, the medium was DMEM containing 10% fetal bovine serum and 1% penicillin-streptomycin. The fusion degree of cells should be about 80-90%; Two aseptic 1.5ml centrifuge tubes were taken, one of which was added with 6 µg virus skeleton protein vector plasmid, 3 µg envelope protein packaging plasmid, and 3 µg target gene plasmid, which was filled to 1ml with D0 medium, and the other was added with 30 µl Turbofect transfection reagent for lentivirus packaging. The cells are sent back to the incubator for 2 days (36-48 hours), and all the supernatant are collected into a 15ml centrifuge tube; At a low temperature of 4 °C, 400g was centrifuged for 5 minutes and then centrifuged supernatant was filtered with a 0.22 um PVDF bacterial filter. The supernatant was added with Lenti-X 10 × and incubated at 4 °C for 4-8h; Centrifuge it at 4 °C for 45 minutes, re-suspend it with 100uLR0, and store it at -80 °C for later use.

2.5 T Cell Transduction of Lentivirus

The isolated T lymphocytes were spread on a 96-well U base plate, with 5×10^5 cells per well and 100uL medium; Take 50uL virus stock solution and add 1000g per well, centrifuge for 1 hour. After the centrifuge, carefully discard the upper culture solution, replace it with 200uL/well fresh culture medium, and put it in a constant temperature incubator setting at 37 °C, CO₂, 5% to observe the positive rate after 48 hours.

2.6 Flow Cytometry Detection

Because the detection objects in this paper are spontaneous green fluorescence or red fluorescence samples, there is no need to carry out the staining step of fluorescein coupled antibody. Take 2E5/part of the cells to be detected directly to 1.5 ml EP tube, add 1mlDPBS to wash, 500g,

centrifuge for 5min, and then add 200ul DPBS to re-suspend the cell mass. In other words, we should make preparations before the sample flow cytometry is put into operation. Use BD Fortessa flow cytometry, set software and fluorescence parameters, and choose AF488 or FITC channel to detect green fluorescent protein. Moreover, we choose the PE-Texas Red channel to detect red fluorescent protein, adjust the forward angle and lateral angle according to the cell size, and adjust the appropriate excitation photovoltage. In this paper, AF488-500V and PE-Texas Red-550V are used. We need to set the cell gate, read and record the data, and use Flowjo 10 flow cytometry analysis software to analyze the data and draw the data map.

2.7 Real-Time Cellular Analysis (RTCA)

100ul of RPMI1640 suspension cell culture medium was added to each well, and the base parameters were adjusted in RTCA data software. According to $1E4$ /well density, the target cell is non-small cell lung cancer of cell line A549 was laid in the RTCA circuit orifice plate. Meanwhile, the circuit orifice plate was placed in the RTCA machine hole position, and time point 1 gating was set; After 24 hours, four experimental groups were set up, and three effect-target ratios were added, namely, conventional T lymphocyte: A549=1:1, CD19-CART cell: A549=1:4, 1:1, 4:1 respectively. The circuit orifice plate was placed in the RTCA machine hole, and the time point 2 gating was set. After 48 hours, the experiment was terminated and the experimental results were derived.

3. Experimental Results

3.1 Codon Optimization of CD19-CAR Target Gene

Firstly, we designed the skeleton of the chimeric antigen receptor through a literature search, including a signal peptide, CD19 antibody recognition domain, transmembrane domain, costimulatory domain, and signal transduction domain. Then, we added the reporter gene EGFP sequence and used the EF-1 α promoter to express the target gene. After designing the complete sequence, we optimized the codon of the whole sequence. Fig. 1A shows codon preference optimization to make the relative adaptability of sequence codons distributed along the length of the gene sequence. From the perspective of gene expression level, the codon adaptation index (CAI) of 1.0 is considered the most ideal expression vector, and a CAI of 0.9 is considered a very good expression vector. After sequence optimization, our CAI reaches 0.95. Fig. 1B shows the optimization of the GC codon content of the sequence. The peak value of GC% content in the 60bp window is taken out, and the ideal percentage range is 30%-70%. Fig. 1C shows the optimized mRNA secondary structure, while Fig. 1D shows the preferred codon frequency. The codon with the highest frequency used by the target organism is set to 100. According to our target expression organism, we optimized according to the mammalian preferred codon.

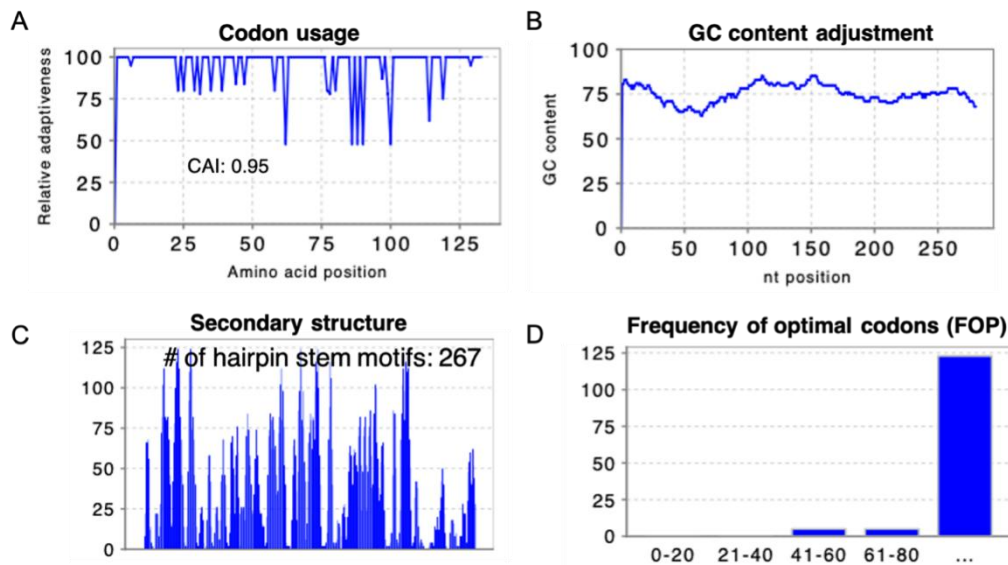


Fig. 1. Optimized Codon Map of CD19 Target Gene.

Vector relative adaptability test, codon adaptation index CAI=0.95;
 Adjust the percentage of codon GC content, and the final GC% is 60%;
 mRNA secondary structure analysis showed that the adjusted hairpin motif was 267;
 Codon preference frequency setting, which sets the frequency of the codon with the highest frequency used by mammals to 100.

3.2 Construction of CD19-CAR and CD19 Protein Overexpression Plasmid

We linked the optimized CD19-CAR sequence of the target gene in 3.1 to an enhanced green fluorescent protein (EGFP) through a lentivirus expression vector to characterize the expression efficiency of the target gene (Fig. 2A); The target gene CD19 was linked to the red fluorescent protein mCherry (Fig. 2B), and the expression vector was constructed to simulate B cells in normal people. Therefore, we packaged the expression vector overexpressing CD19 protein into lentivirus and transduced it into non-small cell lung cancer cell line A549 to test the killing activity of CD19-CART lymphocytes. The method of constructing an expression vector is homologous recombination.

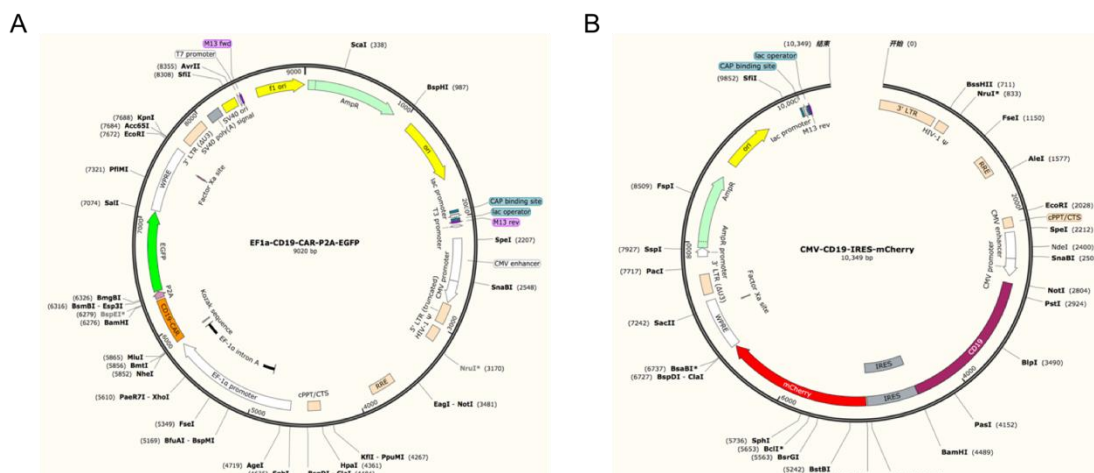


Fig. 2. Construction Map of Target Gene Overexpression Vector.

CD19-CART overexpression vector construction map. Using the EF-1 α promoter, the target gene CD19-CAR was linked to the reporter gene EGFP through hopping peptide P2A, and the vector resistance was Amp ampicillin resistance.

B. Construction of CD19 gene overexpression vector map. Using the CMV promoter, the target gene CD19 was linked with the reporter gene mCherry by linking peptide IRES, and the vector resistance was Amp ampicillin resistance.

3.3 Identification of CD19-CAR Plasmid

To verify the CD19-CAR gene-positive plasmid, we identified the constructed target expression vector by double enzyme digestion. The selected restriction endonuclease is NheI and BamHI, and the positive situation of 8 clone vectors was identified by agarose nucleic acid gel electrophoresis. As shown in Figure 3, the leftmost lane is the DNA marker, which is used to indicate the size of nucleic acid fragments. Through the nucleic acid electrophoresis map, we identified 4 correct clones, which are located in lanes 1, 3, 4, and 8 respectively. Unsuccessful clones were located in lanes 2, 5, 6, and 7, with the construction rate of positive clones at 50%.

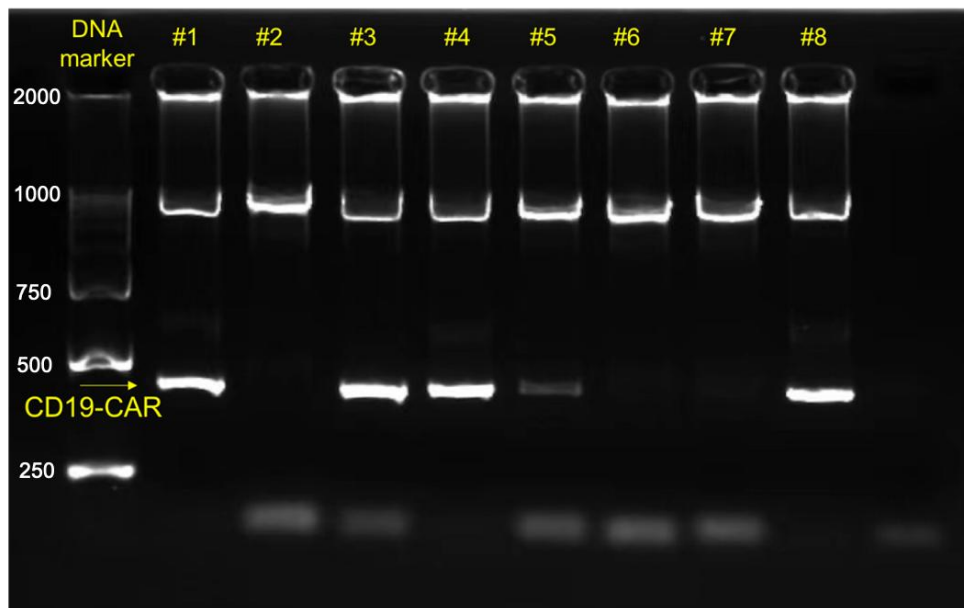


Fig. 3. Identification Diagram of Target Gene by Gel Electrophoresis With Double Enzyme Digestion.

The leftmost lane is the DNA marker, and the clones to be identified are located in lanes # 1-# 8. The arrows indicate the successful target gene fragments.

3.4 Sequencing of CD19-CAR Gene

Four positive clones were identified by double enzyme digestion, and the CD19-CAR gene sequence was sequenced to confirm that there were no mutant bases in the target gene sequence, including base substitution, transversion, deletion mutation, and insertion mutation. We used Sanger sequencing, by incorporating radioactively labeled nucleotide analogues, and the DNA fragments separated by agarose gel electrophoresis were identified. The identification results are shown in Fig. 4 (showing 1-315bp). Through sequence alignment, it was identified that the gene sequences of # 1, # 3, and # 4 clones were correct. Meanwhile, the base peak map was single and clear, and the # 8 clone had a deletion mutation at base 565, so it was discarded. In the follow-up experiment, clone # 1 was selected for testing.

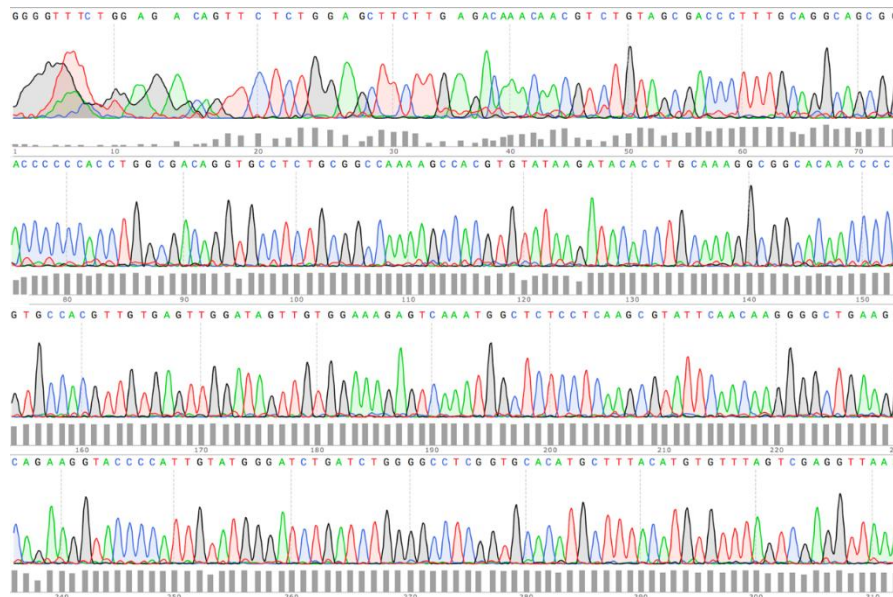


Fig. 4. Sequencing Results of CD19-CAR Gene. Here is a sequencing map of the first 315bp of clone # 1 of the CD19-CAR gene.

3.5 Packaging of CD19-CAR Lentivirus and CD19 Lentivirus Transduction

We selected the HEK293T cell line for CD19-CAR lentivirus packaging. Figure 5A (left) shows the bright field image of the 293T cell line under a microscope, which shows that 293T is an adherent cell line, and the conjugation density of cells during virus packaging is roughly 70-80%. We used the plasmid of the # 1 target gene identified in 3.3 and the plasmid of the # 2 control empty to package lentivirus. Fig. 5B (left) shows a fluorescence microscope image 48 hours after transfection of # 2 control empty plasmid. It can be seen that the cells do not emit fluorescence under the excitation of a green laser. Fig. 5B (right) shows the 48h fluorescence microscope image after transfection of the # 1 target gene plasmid. After transfection of CD19-CAR-EGFP plasmid, 293T can emit fluorescence under the excitation of a green laser, indicating that the cells successfully express the CD19-CAR target gene.

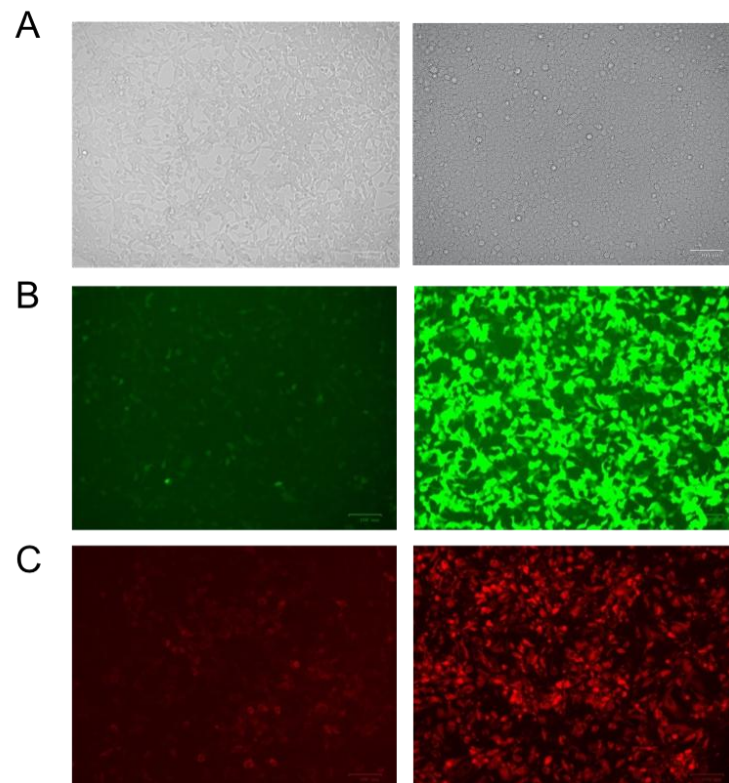


Fig. 5 Image of Lentivirus Transduction in HEK293T Cells Under Fluorescence Microscope.

We packaged lentivirus with CD19 gene expression vector in the HEK293T cell line. The method is the same as CD19-CAR-EGFP, and the packaged lentivirus was transduced into the A549 tumor cell line. The bright field is shown in Fig. 5A (right), while Fig. 5C (left) is the transduction image of the control lentivirus packaged with a no-loaded plasmid. Fig. 5C (right) is the transduction image of the CD19-mCherry target plasmid, which shows that lentivirus has high transduction efficiency.

Fig. 4A is a bright field microscopic image of the HEK293 and A549 tumor cell lines respectively; Fig. 4B is a fluorescence microscopic image (EGFP) of the HEK293 lentivirus package;

Fig. 4C is a fluorescence microscopic image (mCherry) of the CD19 lentivirus transduced A549 tumor cell line.

3.6 CD19-CAR T Lymphocyte Identification by Flow Cytometry

In order to quantitatively analyze the transduction efficiency of CD19-CAR lentivirus to T lymphocytes, we detected the positive rate of cell transduction under different lentivirus MOI by flow cytometry. As shown in Fig. 6, when MOI=0, the ratio of EGFP expression in T lymphocytes was 4.00%. When MOI=10, the ratio of EGFP expression increased to 51.3%. When MOI=20, the ratio of EGFP expression in T lymphocytes was the highest, which was 74.5%. It can be seen that the positive rate of CD19-CAR lentivirus infection increases linearly with the increase in the number of CD19-CAR lentivirus infections.

From left to right, lentivirus transduction flow cytometry data with elevated MOI were obtained. The abscissa is the reporter gene EGFP, and the ordinate is forward angle FSC-H.

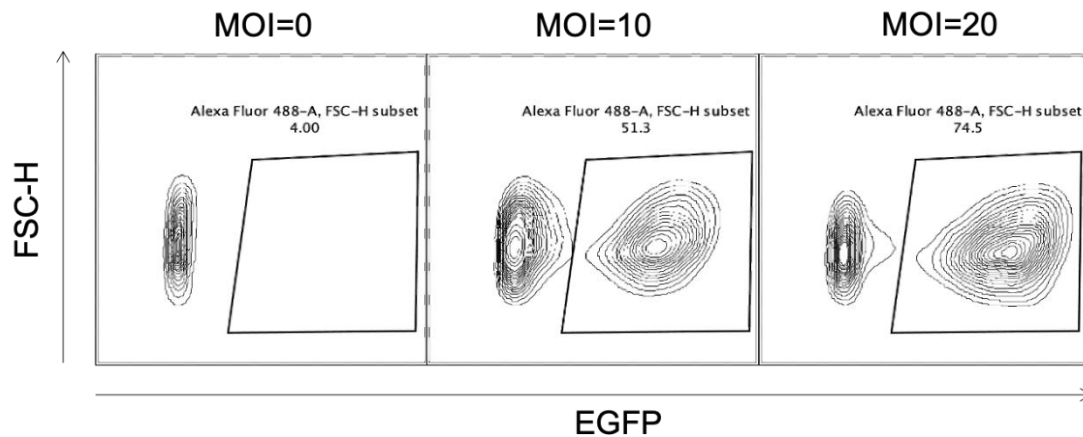


Fig. 6. CD19-CAR Lentivirus Transduces T Lymphocytes.

3.7 CD19-CAR T Lymphocytes Killing Tumors

In order to observe the tumor-killing ability of CD19-CART lymphocytes more intuitively, we used real-time cellular analysis (RTCA) to characterize it. We set up five experimental groups, namely A549-CD19 tumor cell line alone and CD19-CART lymphocytes with different ratios at the same time, with the effect-target ratio of 1:4, 1:1, and 4:1. Meanwhile, we also set up a group of conventional untransduced T lymphocytes as control. Results are as shown in fig. 7. The A549-CA19 tumor cell line alone continued to proliferate with the extension of observation time. In the experimental group with CD19-CART lymphocytes, the proliferation index of tumor cells decreased significantly, and the decline rate of the proliferation index increased significantly with the increase of the effect-target ratio. It is worth noting that the effect-target ratio of conventional untransduced common T lymphocytes in the experimental group was 1:1 (yellow curve). Besides, under this effect-target ratio, the killing activity for the tumor is far less than the 1:4 (dark blue curve) of CD19-CART. Therefore, it fully reflects that the ordinary unmodified T lymphocytes of the body are disabled in killing and recognizing tumors. In contrast, the advantages of chimeric antigen receptor technology are obvious. This experiment intuitively shows the strong dynamic tumor-killing activity of CD19-CART lymphocytes.

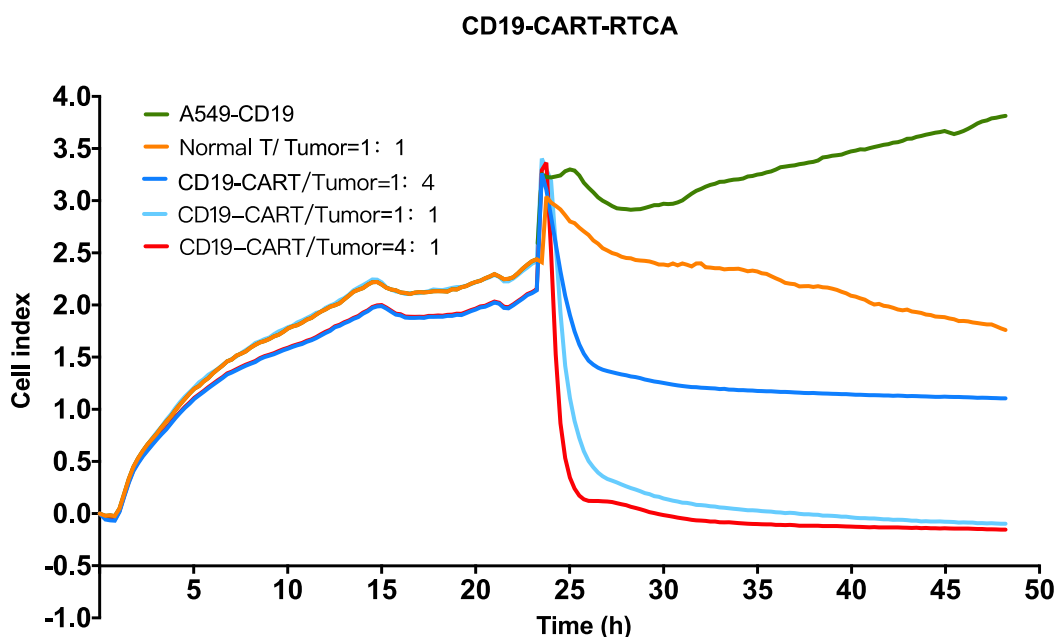


Fig. 7. Verification of CD19-CART Lymphocyte Killing Activity.

The abscissa of the data graph is the observation time (hours), and the ordinate is the cell proliferation index. The green curve shown in the figure is the proliferation curve of A549-CD19, the yellow curve is the proliferation curve of conventional untransduced common T lymphocytes with an effect-target ratio of 1:1; the dark blue curve is the proliferation curve with an effect-target ratio of 1:4, the light blue curve is the proliferation curve with an effect-target ratio of 1:1, and the red curve is the proliferation curve with an effect-target ratio of 4:1.

4. Experimental Conclusion and Prospect

In this paper, chimeric antigen receptor T immune cells targeting hematological malignant tumors of acute B-cell lymphoma were designed and constructed to kill tumor cells specifically and efficiently. The innovative technology adopted in this paper can visually and real-time observe the dynamic killing activity of CART cells in vitro, and ordinary T lymphocytes without transduction were used as an experimental control. Through experimental verification, the following conclusions are drawn. CD19 chimeric antigen receptor T cells have significant killing activity for targeting tumors and are far stronger than ordinary unmodified T lymphocytes.

CART cell therapy technology has a very broad development prospect in tumor treatment. But at the same time, it is undeniable that CART cell technology also faces many problems. For example, most tumors still lack good therapeutic targets; Some existing tumor-associated antigens that can be targeted also show a certain low level of expression in normal cells, resulting in “targeted, non-tumor” toxicity; In addition, because CART technology is a virus-based expression system, the biosafety of therapy needs further observation.

How to better solve the above problems will have an important influence on the development of CART cell therapy technology. The development of biological science is changing all the time. CRISPR and CART have become hot technologies in the field of life science. The advantages of combining gene editing artifacts with the new generation of cellular immunotherapy have gradually become prominent. With the help of CRISPR-Cas9 technology, the development of CART will enter a new stage. In addition to technical cooperation, the challenges of CART technology mainly lie in the selection of target antigens, the overcoming of tumor immunosuppressive microenvironment, and the control of toxicity. Using new biological technologies to further strengthen this tripod will make CAR drive faster and more stable.

5. References

- [1] Xia, C., et al. Cancer statistics in China and United States, 2022: profiles, trends, and determinants. *Chinese medical journal* 135, 584-590 (2022).
- [2] Sterner, R.C. & Sterner, R.M. CAR-T cell therapy: current limits and potential strategies. *Blood cancer journal* 11, 69 (2021).
- [3] MacDonald, K.G., et al. Alloantigen-specific regulatory T cells generated with a chimeric antigen receptor. *The Journal of clinical investigation* 126, 1413-1424 (2016).
- [4] Jin, C., Yu, D. & Essand, M. Prospects to import chimeric antigen receptor T-cell therapy for solid tumors. *Immunotherapy* 8, 1355-1361 (2016).
- [5] Bezverbnaya, K., Mathews, A., Sidhu, J., Helsen, C.W. & Bramson, J.L. Tumor-targeting domains for chimeric antigen receptor T cells. *Immunotherapy* 9, 33-46 (2017).
- [6] Fesnak, A.D., June, C.H. & Levine, B.L. Engineered T cells: The promise and challenges of cancer immunotherapy. *Nature reviews. Cancer* 16, 566-581 (2016).
- [7] Kuramitsu, S., et al. Adoptive immunotherapy for the treatment of glioblastoma: progress and possibilities. *Immunotherapy* 8, 1393-1404 (2016).
- [8] Dutoit, V., Migliorini, D., Dietrich, P.Y. & Walker, P.R. Immunotherapy of Malignant Tumors in the Brain: How Different from Other Sites? *Frontiers in oncology* 6, 256 (2016).

- [9] Jackson, H.J., Rafiq, S. & Brentjens, R.J. Driving CAR T-cells forward. *Nature review. Clinical oncology* 13, 370-383 (2016).
- [10] Sotillo, E., et al. Convergence of Acquired Mutations and Alternative Splicing of CD19 Enables Resistance to CART-19 Immunotherapy. *Cancer discovery* 5, 1282-1295 (2015).
- [11] Turtle, C.J., et al. CD19 CAR-T cells of defined CD4 +: CD8 + composition in adult B cell all patients. *The Journal of clinical investigation* 126, 2123-2138 (2016).
- [12] Huang, R., et al. Recent advances in CAR-T cell engineering. *Journal of Hematology & Oncology* 13, 86 (2020).
- [13] Westin, J.R., et al. Effectiveness and safety of CD19-directed CAR-T cell therapies in patients with relapsed/refractory progressive B-cell lymphomas: Observations from the JULIET, ZUMA-1, and TRANSCEND trials. *American journal of hematology* 96, 1295-1312 (2021).
- [14] Zhang, Q., et al. CAR-T Cell Therapy in Cancer: Tribulations and Road Ahead. *Journal of Immunology Research* 2020, 1924379 (2020).
- [15] Wang, Z., Wu, Z., Liu, Y. & Han, W. New Development in CAR-T Cell Therapy. *Journal of Hematology & Oncology* 10, 53 (2017).